Int. J. Nano Dimens., 8 (4): 274-283, Autumn 2017

ORIGINAL ARTICLE

Room temperature dielectric and antibacterial behavior of thiosemicarbazide capped low dimension Silver and Gold nanoparticles

Bhagavathula S. Diwakar[1*]; Boddeti Govindh[2]; Devarapu Chandra Sekhar[1]; Penmetsa Bhavani[1]; Veluri Swaminadham[3]; Kondareddy Anji Reddy[1]

[1]Department of Engineering Chemistry, SRKR Engineering College, Chinna Amiram, India
[2]Organic Research Lab, Department of Organic Chemistry, Andhra University, Visakhapatnam, India
[3]Department of Physics, Swarnandhra College of Engineering and Technology, Narsapur, A. P., India

Received 07 June 2017; revised 27 August 2017; accepted 06 September 2017; available online 11 September 2017

Abstract

Room temperature dielectric and antibacterial behavior of thiosemicarbazide capped low dimension Silver and Gold nanoparticles were studied. The effect of size on the properties, by capping silver (Ag) and gold (Au) nanoparticles by thiosemicarbazide (TSC) was investigated. The nanoparticles were synthesized by chemical reduction method. The structural formation, surface morphology, phase stability and crystalline nature were characterized by UV-Vis spectroscopy, Fourier transform Infra Red (FT-IR) spectroscopy, Differential scanning calorimeter (DSC), Scanning Electron Microscopy (SEM), Transmission Electron Microscopy (TEM) and Powder X-ray diffraction (PXRD). Room temperature dielectric and Impedance spectroscopy were performed to understand the electrical transport behavior and the results indicated that TSC capped Ag nanoparticles have demonstrated better electrical properties. Also, antibacterial studies were performed on human pathogenic bacteria by agar well diffusion method which attested TSC capped Ag nanoparticles have better antibacterial properties.

Key words: *Anti bacterial; Capping; Dielectric; Impedance spectroscopy; Silver and Gold nanoparticles; Thiosemicarbazide.*

How to cite this article

Diwakar BS, Govindh B, Chandra Sekhar D, Bhavani P, Swaminadham V, AnjiReddy K. Room temperature Dielectric and antibacterial behavior of thiosemicarbazide capped low dimension Silver and Gold nanoparticles. Int. J. Nano Dimens., 2017; 8 (4): 274-283.

INTRODUCTION

Metal nanoparticles (Ag, Au) have renowned applications in basic sciences due to their distinct optical, electrical and photo thermal applications [1-8]. Silver and Gold nanoparticles showed conductivity, chemical stability, catalytic, antibacterial activity and also act as an ideal candidate for molecular labeling because of their large operative scattering cross section and surface plasmon resonance [9-12]. It is well studied that silver nanoparticles were extensively utilized to exploit their novel properties such as antibacterial, catalysis and bio-sensing and their toxicity and possible cancer risk [13-20]. The flexibility in synthesizing the Ag and Au nanoparticles makes them attractive candidates for research. Metal nanoparticles were generally synthesized by different protocols such as chemical [21], electrochemical [22], chemical vapor deposition [23], photochemical, molecular beam epitaxy [24] and chemical reduction [25, 26] by various stabilizing agents. It is important to note that, the interaction of metal precursor ions with reducing agents and capping agent can greatly affect the size, shape, stability and physiochemical properties of the metal nanoparticles [27, 28]. Therefore the selection of an appropriate capping agent is a constraint for stabilizing nanoparticles. Capping agents can work by a variety of mechanisms, including electrostatic

* Corresponding Author Email: *bsd2020@gmail.com*

stabilization, steric stabilization, hydration forces, depletion stabilization and stabilization using van der Waals forces [29] and the combination of these mechanisms. Apart from stabilizing the nanoparticles, capping agents can play the additional role of reducing metal nanoparticles.

Literature rich studies on the silver and gold nanoparticles with different stabilizing and capping agents such as thiols [30-32], amine functionalized compounds [33], acids [34], alcohols [35] and different polymer capping agents [36]. For example silver nanoparticles were stabilized by cysteine at pH >8 but at pH < 7 causing silver nanoparticles aggregation [37, 38]. Thiosemicarbazide (TSC) and its derivatives were showing better chelating ability. Apart from stabilizing the metal nanoparticles, the thiol and amine groups may from different side products in their synthesis. So it was necessary to understand the metal and capping agent interactions to derive the most suitable mechanism for the formation of stable metal nanoparticles.

Hence, it was focused on synthesizing stable silver and gold nanoparticles by stabilizing with TSC. In this study, the synthesis and morphology of thiosemicarbazide-capped silver and gold nanoparticles were achieved by utilizing a simple chemical reduction of metal iodide employing sodium borohydride. The advantage of this method was ease of preparation, convenience in use and especially, the obtained nanoparticles were uniform in their shape and size. UV-vis spectroscopy, SEM and TEM were employed to monitor the formation process of metal nanoparticles. This may be helpful in understanding the growth of nanoparticles and creates a new dimension in controlling the shapes of nanoparticles. Furthermore, room temperature electrical impedance spectroscopy, room temperature dielectric behavior and their antibacterial properties on three different human pathogenic bacteria species were investigated.

EXPERIMENTAL

Synthesis of Thiosemicarbazide capped Silver nanoparticles

A total of 2.5 mL of 10^{-2} M $AgNO_3$ was added to 75 mL of triply distilled organic-free water. A total of 5 mL of 10^{-2} M thiosemicarbazide (dissolved in hot water) was added as stabilizer to the above solution with stirring. After 10 min of mixing, 2.5 mL of 10^{-2} M potassium iodide (KI) was dropped into the solution slowly, yielding a green yellow AgI colloid. A total of 20 mg of $NaBH_4$ was added to AgI colloidal solution, and the reaction mixture was continually stirred for about 20 min. The silver colloid was finally obtained. During the whole reaction, colour of the colloidal solution changed from green-yellow to nut-brown at beginning, then to brown, and finally to black.

Synthesis of Thiosemicarbazide capped Gold nanoparticles

A total of 2.5 mL of 10^{-2} M Chloro Auric acid was added to 75 mL of triple distilled organic-free water. A total of 5 mL of 10^{-2} M thiosemicarbazide (dissolved in hot water) was added as a stabilizer to the above solution with stirring. After 10 min of mixing, 2.5 mL of 10^{-2} M potassium iodide (KI) was dropped into the solution slowly, yielding a green yellow AuI colloid. A total of 20 mg of $NaBH_4$ was added to the AuI colloidal solution, and the reaction mixture was continually stirred for about 20 min. The gold colloid was finally obtained. During the whole reaction, the colour of the colloidal solution changed from yellow to dark red at the beginning, then to brown, and finally to black.

Antimicrobial studies and Determination of Zone of Inhibition

Anti-bacterial studies are performed on *Salmonella typhi, Vibrio cholera, Shigella dysentery*; species are collected and isolated from blood and fecal samples of infected patients at King George Hospital, Visakhapatnam. Microscopic observations, cultural characteristics, and biochemical tests were performed for organism identification [39, 40].

Zone of inhibition was determined by agar well diffusion method [41]. Sterilized agar medium (MHA for bacteria, SDA for dermatophyte) poured into Petri plate with inoculum by subsurface pour plate method. A 6mm well was cut in the center of each plate using a sterilized cork borer. 50 µl of compound and Antibiotic (Griseofulvin) for dermatophyte fungi, Ciprofloxacin for bacteria as positive control were placed into the wells. Bacteria inoculated plates were incubated at 34^0C for 24 hours. Fungal inoculated plates were incubated for 5 days at 28 ^{0}C for the observation of zones of inhibition. Zone of inhibition was expressed in milli meter with Himedia zone reader. The experiments were conducted according to Clinical and Laboratory Standards Institutes [42, 43].

Impedance spectroscopy

Electrochemical Impedance Spectroscopy (EIS) studies were carried out on Novocontrol Alpha A Impedance Analyzer under the frequency range 1Hz-1 MHz with 10 mV applied ac voltage at room temperature. The synthesized powders were made into pellets 10 mm (TSC-AgNp) and 6 mm (TSC-AuNp) and then connected in parallel to the electrode with conductive silver paint on both sides.

RESULTS AND DISCUSSIONS

At first, the nanoparticles formation was identified by the absorption spectra. They results were presented in Fig. 1. The spectra were recorded in distilled water medium. The optical absorption spectra of metal nanoparticles were dominated by surface Plasmon resonances (SPR), which shift to longer wavelengths with increasing particle size [44]. After addition of precursor salt solution to potassium iodide solution, the colour of the solution changes from colourless to light yellow (for $AgNO_3$ solution) and golden yellow to lemon yellow (for $HAuCl_4$ solution) indicated the nucleation of the metal particle at the infancy. After adding the thiosemicarbazide and $NaBH_4$, the reaction started and the colour of the solution turned into black which confirmed the formation of nanoparticles. From UV data, the surface plasmon absorption of silver nanoparticles have shorter wavelength band in the visible region at 432 nm and for the gold nanoparticles the band appeared at 535 nm indicated the polydispersion of formed metal nanoparticles with the reduction in its size [45].

Further structural analysis was performed by DSC analysis and the results were presented in Fig. 2. An endothermic peak can be observed by increasing the temperature in the DSC thermograms of the samples obtained by thermal treatment of thiosemicarbazide. In addition, the DSC measurement provided a confirmation for the presence of thiol-capped silver nanoparticles into the prepared samples. The DSC thermogram of the sample obtained by thermal decomposition of TSC capped Ag showed three different endothermic peaks. The peak at the lower temperature corresponded to the collapse of $–NH_2$ groups present in the organic capping layer, whereas the second peak at the higher temperature can be attributed to the collapse of the interaction between thiol & amine groups on neighbor nanoclusters. Table 1 lists the temperature range of the endothermic peaks and the enthalpy values in the examined phase transitions. The FTIR spectrum (presented in ESI) of the nanocrystals provides additional information about the local molecular environment of thiosemicarbazide. It was noted that there was an observable change in the C=S, $-NH_2$ vibrations which confirmed us that the metal nanoparticles were attached to the sulfur and amine group especially which is supported by the DSC data in which the breaking of C=S, amine groups occurs at high temperature.

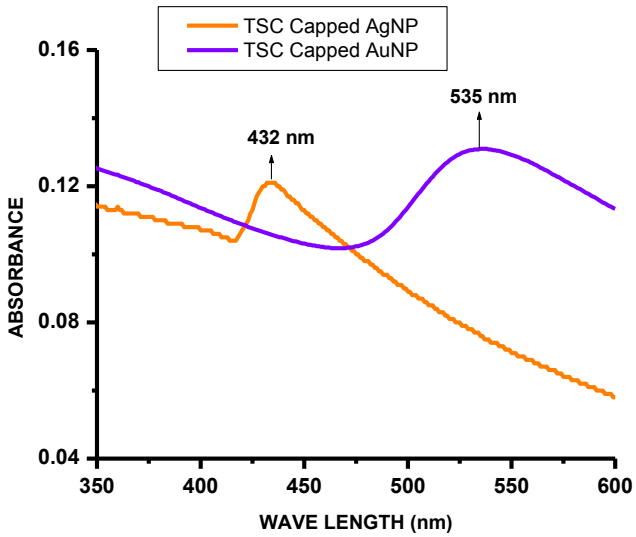

Fig. 1: UV-Visible spectral studies of thiosemicarbazide capped silver & gold nanoparticles.

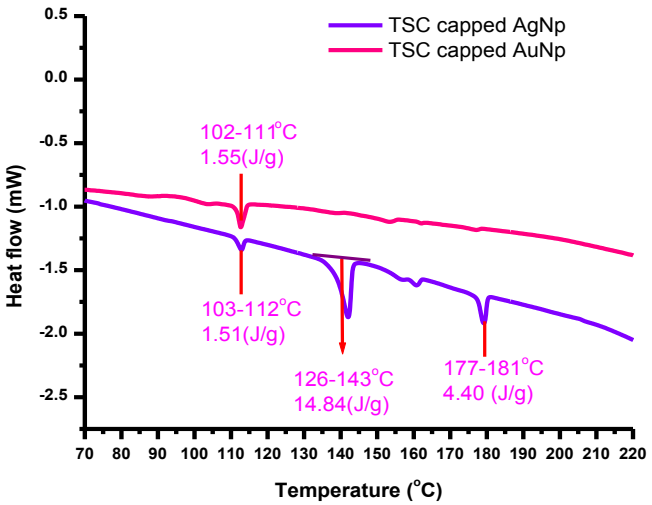

Fig. 2: DSC-thermograms of samples obtained by thermal decomposition of thiosemicarbazide capped AgNp & AuNp.

Table 1: DSC analysis of thiosemicarbazide capped Agnp & Aunp.

S.No	Sample	Order-Disorder Temperature (°C)	Δh(J/g)
1	TSC cappedAgNp	103-112	1.51
		126-143	14.84
		177-181	4.40
2	TSC capped AuNp	102-111	1.55

The reason for the intensity difference between the spectra was believed to be the thiolate molecules on the nanoparticles forming a relatively closely packed thiol layer and molecular motion being constrained [46, 47]. Thus, this steric constraining effect on the transverse mode was stronger than that on the longitudinal mode. Therefore, the change of the peak intensity in the longitudinal modes is smaller than that of the transverse mode. The noted IR vibrations for $–NH_2$, C=S, C–S groups in TSC, TSC capped Ag and TSC capped Au nanoparticles are 3374, 3424, 3445; 1626, 1614, 1546, 800, 842 and 875 cm^{-1} respectively.

Fig. 3 represented the XRD pattern of powder silver and gold nanoparticles. The presence of peaks at 2θ values 38.1, 46.40 and 64.5 corresponds to (1 1 1), (2 0 0) and (2 2 0) planes of silver respectively and 38.31, 47.68 and 67.74 corresponds to (1 1 1), (2 0 0) and (2 2 0) planes of gold respectively. Thus the XRD spectrum confirmed the crystalline structure of TSC capped metal nanoparticles. The other peaks were organic impurities. All the peaks in XRD pattern can be readily indexed to face-centred cubic structure of silver as per available in literature. The average size of the nanoparticles was calculated from XRD data according to the line width of the maximum intensity reflection peak by using the Scherrer's equation. It is well known that with diminishing crystallite size, the measured XRD pattern exhibits broadening, and very often overlapping reflections. The broadening of the reflections is inversely proportional to the crystallite size (i.e. size of coherently diffracting domains). From the obtained spectrum the size of the silver nanoparticles were calculated as 15.2 nm. The average size of the gold nanoparticles was calculated from the XRD data according to the line width of the maximum intensity reflection peak by using the Scherrer's equation and it is 20 nm.

The SEM images for gold & silver nanoparticles were presented in Fig. 4a, 4b respectively. Form these figures it was observed that the formed nanoparticles were crystalline in nature with certain degree of porosity. It was observed that the silver nanoparticles were scattered over the surface and no aggregation was noticed but gold nanoparticles were aggregated over the surface.
Silver & Gold nanoparticles were further examined using transmission electron microscopy (TEM).

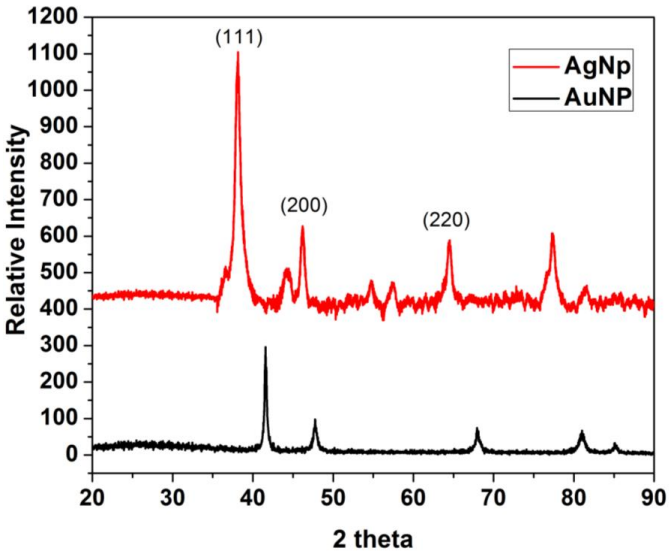

Fig. 3: XRD patterns of TSC capped AgNp and AuNp.

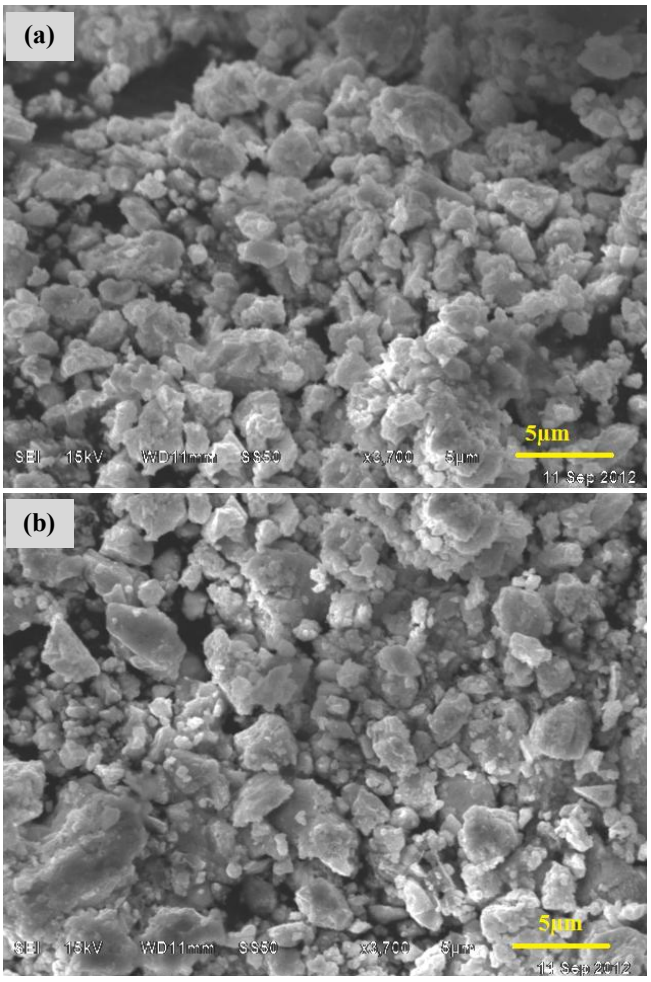

Fig. 4: a) SEM image of TSC-AgNp, b)SEM image of TSC-AuNp.

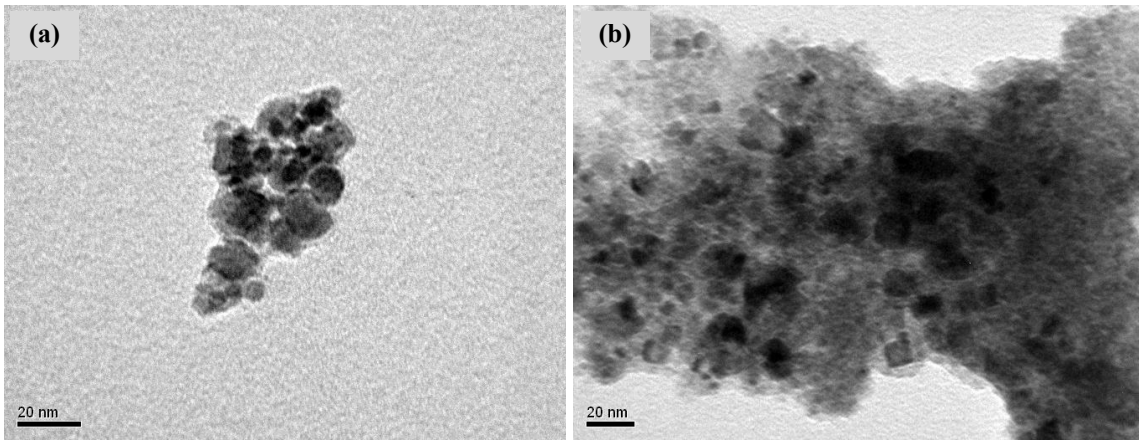

Fig. 5: a) TEM image of TSC-AgNp, b) TEM image of TSC-AuNp.

The TEM images of synthesized silver and gold nanoparticles were recorded and presented in Fig. 5a, 5b. The average size of silver and gold nanoparticles was in agreement with Scherer's equation.

Room temperature dielectric Studies

The dielectric studies of the materials are very important to know the transport mechanism and lattice dynamics of the crystalline material. It also provides information about the nature of the atom, ion, bonding and their polarization mechanism. According to the IR and DSC studies, the nanoparticles were expected to bind to the sulfur group and the terminal -NH_2 group of thiosemicarbazide and thus stabilized. The dielectric constant (ε') value of a material depends on the amount of mobile (polarizable) electrical charges in it and the degree of mobility of these charges. When a current flows across the two-material dielectric interfaces, charges accumulate at the interface with different relaxation times. This is possible because of the presence of a moderate number of charge centres and carrier centres on the surface, which forms a capacitor network to store energy. From Fig. 6a**,** it was observed that the ε' of the TSC caped AgNp is higher than that of the TSC caped AuNps. This may be attributed to the tendency of dipoles. If the dipoles were oriented in the direction of applied frequency, they show better dielectric behaviour. In this case, dipoles of TSC caped AgNp and AuNp were oriented in the low-frequency range. It was also noted that the ε' value has two different regions: the first, representing an exponential increase in a low frequency below 1000 Hz, and the second showing a linear relation between the frequency and the ε' value in the range of high frequency above 1000 Hz. This was related to the rotational movement of functional groups in the samples, which can be decelerated at a higher frequency. According to Maxwell-Wagner polarization theorem, the material with large grain boundaries can affect the electric conduction [48]. Therefore, grain boundary volume/ grain boundary interfacial polarization controls the behaviour of dielectric constant at low frequencies. A material with low dielectric loss can be used as better capacitors in energy storage. The dielectric loss factor was presented in Fig. 6b, the TSC caped AuNp's showed low dielectric loss than TSC capped AgNp's. These results were in good agreement with the dielectric constant. The behaviour of dielectric loss in the low-frequency range depends on many factors like defects, the size of the crystallite. Hence, in TSC caped AgNp's and AuNp's the crystallite possess a lesser number of electrically active defects. This kind of phenomena was observed in non-linear optical materials.

Furthermore, EIS experiments were performed in the frequency range between 1 Hz and 1MHz with AC voltage amplitude of 10 mV on Novocontrol Alpha A Impedance Analyzer at room temperature. Initially, the powdered materials were made into pellets by using the hydraulic pressure machine. The diameters of the silver and gold pellets were 10 mm & 6mm respectively. The thicknesses of silver & gold pellets were found by using venire calipers as 0.61mm & 0.32 mm respectively.

Fig. 7 showed the Nyquist plots of impedance at room temperature in the frequency range 1Hz-1MHz. The EIS was used to investigate the electron transfer ability of AgNp's and AuNp's. From the Fig. 7, it was observed that the imaginary impedance (Z") versus the real impedance (Z') showed a semicircle and the diameter of TSC caped AgNp impedance graph was lower than that of TSC capped AuNp suggests that TSC capped AgNp $(0.32349 X10^{-6} mho - m^{-1})$ have better electrical conductivity than TSC capped AuNps $(0.27797 X10^{-6} mho - m^{-1})$. Besides that, it was also confirmed that charge transfer resistance was reduced on the TSC and AgNp surface. Therefore these results can be applied to a modified sensor for electrochemical analysis systems.

Antibacterial Studies

Further, the *in vitro* antibacterial activity of the TSC capped silver & gold nanoparticles was performed on three different bacterial strains viz., *Salmonella typhi*, *Vibrio cholera* and *Shigella dysentery* at three different concentration levels (25, 50 and 100 µg/ml) with Ciprofloxacin as a positive control. The activity was reported by measuring the diameter of inhibition zone in mm. and the results were presented in Table 2. From the table, it was observed that thiosemicarbazide capped silver nanoparticles were showing better potency than gold nanoparticles. The antimicrobial activity of thiosemicarbazide capped silver & gold nanoparticles, thiosemicarbazide indicated the size effect on the antibacterial effects. However, the mechanism is still unlocked.

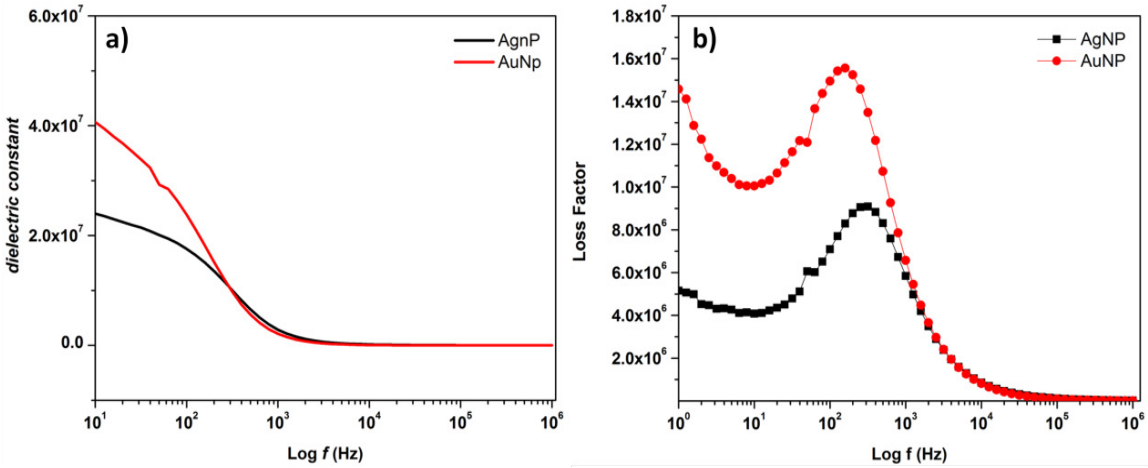

Fig. 6: Room temperature dielectric behaviour of TSC capped AgNp's and TSC capped AuNp's.

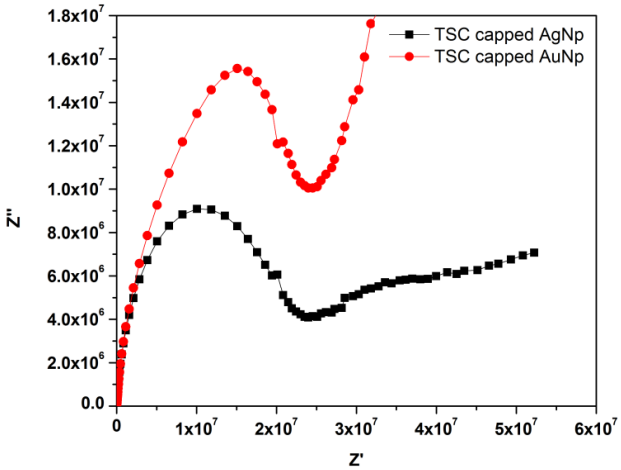

Fig. 7: Nyquist plots of TSC capped Silver and Gold nanoparticles at room temperature.

Table 2: Zone of inhibition (in mm) of capped nanoparticles by agar well diffusion method.

S.No	Compound	Concentration of compound (µg/ml)	*Salmonella typhi*	*Vibrio cholera*	*Shigella dysenteria*
1	Thiosemicarbazide (TSC)	25	9	15	18
		50	15	10	15
		100	20	18	22
2	TSC capped AgNp	25	8	11	10
		50	10	12	13
		100	15	17	20
3	TSC capped AuNP	25	7	13	10
		50	12	14	12
		100	18	20	23
4	Ciprofloxacin	100	25	32	30

CONCLUSION

In this scientific paper, synthesis of thiosemicarbazide capped silver and gold nanoparticles was achieved by chemical reduction method and the particles were well characterized by advanced spectral techniques UV-Visible, FT-IR, PXRD, SEM and TEM. In addition, electrical AC impedance studies revealed the conductive nature of the TSC capped materials. The results demonstrated that the conductivity was through grains and synthesized materials exhibit semiconductor phenomena which can have application in the field of nonlinear optical devices and in electrochemical sensors. Further, the antimicrobial activity of the synthesized nanoparticles was examined and the results showed that TSC capped silver nanoparticles exhibited moderate activity than its gold companion. These results support the effect of size and nature of capping on the functional behavior. However, to understand the capping effect on surface modifications on the functional properties of the materials, further investigations are required.

ACKNOWLEDGEMENTS

The authors are thankful to the Principal SRKR Engineering College for his continuous support. The authors are grateful Andhra University for providing spectroscopic facilities. Further, the authors are greatly acknowledged to Y. Nagendra Sastry, GITAM Univesity, for helping in antibacterial studies.

CONFLICT OF INTEREST

The authors declare that there is no conflict of interests regarding the publication of this manuscript.

REFERENCES

[1] Zhang Y., Huang R., Zhu X., Wang L., Wu C., (2012), Synthesis, properties, and optical applications of noble metal nanoparticle-biomolecule conjugates. *Chin. Sci. Bull.* 57: 238–246.

[2] Alshehri A. H., Jakubowska M., Młożniak A., Horaczek M., Rudk D., Free C., Carey J. D., (2012), Enhanced electrical conductivity of silver nanoparticles for high frequency electronic applications. *ACS Appl. Mater. Interfac.* 4: 7007–7010.

[3] Saxena U., Goswami P., (2012), Electrical and optical properties of gold nanoparticles: applications in gold nanoparticles-cholesterol oxidase integrated systems for cholesterol sensing. *J. Nanopart. Res*. 14: 813-818.

[4] Elghanian R., Storhoff J. J., Mucic R. C., Letsinger R. L., Mirkin C. A., (1997), Selective colorometric detection of polynucleotides based on the distance dependent optical properties of gold nanoparticles. *Science*. 277: 1078-1081.

[5] Kuila B. K., Garai A., Nandi A. K., (2007), Synthesis, optical, and electrical characterization of organically soluble silver nanoparticles and their poly (3-hexylthiophene) nanocomposites: Enhanced luminescence property in the nanocomposite thin films. *ACS Chem. Mater.* 19: 5443-5452.

[6] Xu S., Hartvickson S., Zhao J. X., (2008), Engineering of SiO_2-Au-SiO_2 sandwich nanoaggregates using a building block: Single, double and triple cores for enhancement of near infrared fluorescence. *Langmuir*. 24: 7492-7496.

[7] Huang X., Mostaf A., El-Sayed S., (2010), Gold nanoparticles: Optical properties and implementations in cancer diagnosis and photothermal therapy. *J. Adv. Res*. 1: 13–28.

[8] Rentería-Tapia V., Velásquez-Ordoñez C., Ojeda Martínez M., Barrera-Calva E., González-García F., (2014), Silver nanoparticles dispersed on silica glass for applications as photothermal selective material. *Energy Procedia*. 57: 2241-2248.

[9] Lok C. N., Ho C. M., Chen R., He Y. Q., Yu W. Y., Sun H., Tam P. K., Chiu J. F., Che C. M., (2006), Proteomic analysis of the mode of antibacterial action of silver nanoparticles. *J. Proteome. Res.* 5: 916–924.

[10] Mao C. F., Vannice M. A., (1995), Formaldehyde oxidation over Ag catalysts. *J. Catal*. 154: 230–244.

[11] Marambio-Jones C., Hoek E. M. V., (2010), A review of the antibacterial effects of silver nanomaterials and potential implications for human health and the environment. *J.*

Nanopart. Res. 12: 1531–1551.

[12] Wang Y., Wan J., Miron R. J., Zhao Y., Zhang Y., (2016), Antibacterial properties and mechanisms of gold–silver nanocages. *Nanoscale*. 8: 11143-11152.

[13] Shamaila S., Zafar N., Riaz S., Sharif R., Nazir J., Naseem S., (2016), Gold nanoparticles: An efficient antimicrobial agent against enteric bacterial human pathogen. *Nanomaterials*. 6: 71-78.

[14] Teo W. Z., Pumera M., (2014), Fate of silver nanoparticles in natural waters; integrative use of conventional and electrochemical analytical techniques. *RSC Adv*. 4: 5006-5011.

[15] Levard C., Hotze E. M., Lowry G. V., Brown G. E., (2012), Environmental transformations of silver nanoparticles: Impact on stability and toxicity. *Environ. Sci. Technol*. 46: 6900-6914.

[16] Chen S., Gao H., Shen W., Lu C., Yuan Q., (2014), Colorimetric detection of cysteine using noncrosslinking aggregation of fluorosurfactant-capped silver nanoparticles. *Sensor. Actuat. B: Chem.* 190: 673-678.

[17] Lee P. C., Meisel D., (1982), Adsorption and surface-enhanced Raman of dyes on silver and gold sols. *J. Phys. Chem-US.* 86: 3391-3395.

[18] Samberg M. E., Oldenburg S. J., Monteiro-Riviere N. A., (2010), Evaluation of silver nanoparticle toxicity in skin in vivo and keratinocytes in vitro. *Environ. Health Perspect.* 118: 407–413.

[19] AshaRani P. V., Low G. K. M., Hande M. P., Valiyaveettil S., (2009), Cytotoxicity and genotoxicity of silver nanoparticles in human cells. *ACS Nano*. 3: 279–290.

[20] Ajitha B., Reddy Y. A. K., Reddy P. S., (2015), Enhanced antimicrobial activity of silver nanoparticles with controlled particle size by pH variation. *Powder Technol*. 269: 110-117.

[21] Vorobyova S. A., Lesnikovich A. I., Sobal N. S., (1999), Preparation of silver nanoparticles by interphase reduction. *Colloids Surf*. *A*. 152: 375–379.

[22] Satoh N., Kimura K., (1989), Metal colloids produced by means of Gas evaporation technique V. Colloidal dispersion of Au fine particles to hexane, poor dispersion media for metal sol. *Bull. Chem. Soc. Jpn*. 62: 1758–1763.

[23] Li Z., Li Y., Qian X. F., Yin J., Zhu Z. K., (2005), A simple method for selective immobilization of silver nanoparticles. *Appl. Surf. Sci.* 250: 109-116.

[24] Bahnemann W. D., (1993), Ultrasmall metal oxide particles: Preparation, photophysical characterization and photocatalytic Properties. *Isr. J. Chem.* 33: 115-136.

[25] Hongshui W., Xueliang Q., Jianguo C., Shiyuan D., (2005), Preparation of silver nanoparticles by chemical reduction method. *Collo. Surf. A: Phy. Engg. Aspects.* 256: 111-115.

[26] Chunfang Li., Dongxiang Li., Gangqiang Wan., Jie Xu., Wanguo H., (2011), Facile synthesis of concentrated gold nanoparticles with low size-distribution in water: Temperature and pH controls. *Nanoscale. Res. Lett*. 6: 440-448.

[27] Chen W., Cai W., Zhang L., Wang G., (2001), Sonochemical processes and formation of Gold nanoparticles within pores of mesoporous silica. *J. Colloid Interf. Sci.* 238: 291-295.

[28] Sengupta S., Eavarone D., Capila I., Zhao G. L., Watson N., Kiziltepe T., (2005), Temporal targeting of tumour cells and neovasculature with a nanoscale delivery system. *Nature*. 436: 568–572.

[29] Kim K. D., Han D. N., Kim H. T., (2004), Optimization of experimental conditions based on the Taguchi robust design for the formation of nanosized silver nanoparticles by chemical reduction method. *Chem. Eng. J.* 104: 55–61.

[30] Chiara B., Francesco P., Subhrangsu M., Elena M., Silvia N., Ilaria F., Maurizio Q., Maria V. R., Giovanni P., (2014), Gold nanoparticles stabilized with aromatic thiols: Interaction at the molecule–metal interface and ligand arrangement in the molecular shell investigated by SR-XPS and NEXAFS. *J. Phys. Chem. C*. 118: 8159-8168.

[31] Xiaoli Z., Jouliana M., El K., Liangti Q., Liming D., Quan L., (2007), A facile synthesis of aliphatic thiol surfactant with tunable length as a stabilizer of gold nanoparticles in organic solvents. *J. Colloid. Interface Sci*. 308: 381–384.

[32] Chiara B., Carlo M., Ilaria F., Iole V., Maria V. R., Giuliana A., Chiara M., Federica B., Roberto M., Marco R., Settimio M., Giovanni P., (2012), Silver nanoparticles stabilized with thiols: A close look at the local chemistry and chemical structure. *J. Phys. Chem. C.* 116: 19571–19578.

[33] Singh A. K., Mahe T., Singh D. P., Srivastava O. N., (2010), Biosynthesis of gold and silver nanoparticles by natural precursor clove and their functionalization with amine group. *J. Nanopart. Res.* 12: 1667–1675.

[34] Simon R., Diana K., Wolfgang M. Z., Matthias E., (2014), An easy synthesis of autofluorescent alloyed silver–gold nanoparticles. *J. Mater. Chem. B*. 2: 7887-7895.

[35] Isaeva E. I., Kiryukhina S. N., Gorbunova V. V., (2013), Photochemical synthesis of silver and gold nanoparticles in polyhydric alcohols. *Russ. J. Gen. Chem.* 83: 619-623.

[36] Galina F. P., Alexsandr S. P., Nadezhda P. K., Svetlana A. K., Artem I. E., Tamara G. E., Tat'yana V. F., Larisa M. S., (2014), Green synthesis of water-soluble nontoxic polymeric nanocomposites containing silver nanoparticles. *Int. J. Nanomed.* 9: 1883–1889.

[37] Csapo E., Patakfalvi R., Hornok V., Toth L. T., Sipos A., Szalai A., Csete M., Dekany I., (2012), Effect of pH on stability and plasmonic properties of cysteine-functionalized silver nanoparticle dispersion. *Colloid Surf. B*. 98: 43–49.

[38] Li H., Cui Z., Han C., (2009), Glutathione-stabilized silver nanoparticles as colorimetric sensor for Ni^{2+} ion. *Sensor Actuat B: Chem*. 143: 87-92.

[39] Mackie A., Cartney M., (1996), Practical medical microbiology. *Churchill Livingstone Publisher (Elsevier)*: 14: 141-147.

[40] Taplin D., Zaias N., Rebell G., Blank H., (1969), Isolation and recognition of dermatophytes on a new medium (DTM). *Arch. Dermatol.* 99: 203-209.

[41] Perez C., Pauli M., Bazevque P., (1990), An antibiotic assay by the agar well diffusion method. *Acta Biologiae. et Medicine. Experimentalis*. 15: 113-115.

[42] Methods for Dilution Antimicrobial Susceptibility Test for Bacteria That Grow Aerobically; *Clinical Laboratory Standards Institute Approved Standard – Ninth Edition*. 32: 12-20 (2012).

[43] Pfaller M. A., Castanheira M., Diekema D. J., Messer S. A., Moet G. J., Jones R. N., (2010), Comparison of european committee on antimicrobial susceptibility testing (EUCAST)

and E test methods with the CLSI broth microdilution method for echinocandin susceptibility testing of candida species. *J. Clinic. Microbiol.* 48: 1592–1599.

[44] Xiaohua H., Mostafa El-Sayed A., (2010), The optical absorption spectra of metal nanoparticles were dominated by surface Plasmon resonances (SPR). *J. Adv. Res.* 1: 13-28.

[45] Venkata S., K., Susmila A. G., Sucharitha K. V., Sarma P. V. G. K., Sai Gopal D. V. R., (2016), Biofabrication and spectral characterization of silver nanoparticles and their cytotoxic studies on human CD34 +ve stem cells, 3 Biotech. 6: 216-222.

[46] Shengtai H., Jiannian Y., Peng J., Dongxia S., Haoxu Z., Sishen X., Shijin P., Hongjun G., (2001), Formation of silver nanoparticles and self-assembled two-dimensional ordered superlattice. *Langmuir*. 17: 1571-1575.

[47] Lambert J. B., Shurvell H. F., Lightner D. A., Cooks R. G., (1998), Organic structural spectroscopy. *J. Chem. Educ.* 75: 1218-1226.

[48] O'Neill D., Bowman M. R., Gregg J. M., (2000), Dielectric enhancement and Maxwell–Wagner effects in ferroelectric superlattice structures. *Appl. Phys. Lett.* 77: 1520-1528.